Correlative evolutions of ENSO and the seasonal cycle in the Tropical Pacific Ocean

Heng Xiao and Carlos R. Mechoso
Department of Atmospheric and Oceanic Sciences, University of California, Los Angeles, California

Abstract

The correlative evolutions of ENSO and the seasonal cycle in the tropical Pacific Ocean are examined by performing idealized experiments with an ocean general circulation Model (OGCM) of the Pacific basin. The interfacial fluxes of heat and momentum in these experiments are taken from 1) a sixteen-year long simulation in which the OGCM, coupled to an atmospheric GCM, produced realistic ENSO variability, and 2) NCEP reanalysis data corrected by COADS climatology for the twenty-year period 1980-1999. The surface fluxes are decomposed into seasonal and non-seasonal (interannually varying) components. The forcings for the experimental runs are obtained by superimposing those two components with a six-month shift. It is found that the response to the shifting in terms of eastern basin heat content can reach 20-40% of the maximum interannual anomaly in the control runs. The magnitude of the response is event-dependent. Budget analysis of a selected warm event shows that the mechanism responsible is anomalous zonal advection in the equatorial band. Additional OGCM experiments suggest that both locally and remotely forced signals contribute significantly to the difference between the control and shift experiments. An interpretation based on the "delayed oscillator" paradigm and on the equatorial wave-mean flow interaction is given. It is concluded that the correlative evolutions of the seasonal cycle in the upper ocean and ENSO can include significant nonlinear interactions between equatorially trapped waves and the seasonally varying upper ocean mean circulation and thermocline structure.

1. Motivation

A better understanding of ENSO evolution requires a deeper insight into its interactions with the seasonal cycle of the climate system in the Tropical Pacific. Previous ENSO studies with numerical models of intermediate complexity have suggested several

mechanisms for such interactions (e.g., Battisti, 1988, Tziperman et al, 1997), and even argued that they are essential components of the observed interannual variability (Jin, 1996).

Typical intermediate coupled models used in ENSO research, however, only include seasonal variations in the oceanic surface layer and lower atmosphere mean condition. Intermediate models with modifications that allow for considerations of seasonal variations in other features of the upper ocean circulation (e.g., the thermocline), and GCMs capable of producing a realistic seasonal cycle in the upper ocean, have been used to explore the interactions between ENSO and the seasonal cycle in the upper ocean (e.g. An and Wang, 2001; Guilyardi et al, 2003; Vintzileos et al, 1999b).

The primary goal of this study is to evaluate the impact on ENSO evolution of interactions between interannual anomalies and the seasonal cycle in the Tropical Pacific Ocean. We aim, therefore, to assess the importance of processes absent in typical intermediate coupled models of ENSO, and to test hypotheses proposed by works using modified intermediate models and CGCMs. We follow an approach based on uncoupled OGCM simulations. In this framework, we can consider the entire upper ocean. Also, we can modify the phase difference between interannual anomalies and the seasonal cycle of the surface forcing in a relatively simple and "realistic" way.

We start in section 2 with a description of the model and experiment design. Section 3 presents the results of the shift experiments. Section 4 discusses the impact of direct and remote mechanisms on the response to the shift. The conclusions are in section 5.

2. Model and Experiment Design

We use the Pacific basin ($30^oS - 50^oN$) version of the Modular Ocean Model (MOM, v1.1). The model is configured with 27 layers in the vertical; the horizontal resolution is $1/3^o$ in latitude by 1^o in longitude equatorward of 10^o, increasing to 3^o by 1^o at high latitudes. This OGCM coupled to the UCLA atmospheric GCM (version 6.8 with 15 levels in the vertical and a horizontal resolution of 4^o latitude by 5^o longitude) produced a realistic seasonal cycle in the tropical Pacific and ENSO-like variability with reasonable period and amplitude (Yu and Mechoso, 2000).

Our methodology is similar to that used by Xie (1995), except that to force the OGCM we use model-generated or reanalysis fields while he uses idealizations that are symmetric about the equator and zonally uniform. As a first step, we spin up the OGCM by running it for ten years with the mean seasonal surface fluxes from the CGCM simulation. The model is restarted and run for sixteen years using the full surface fluxes from the CGCM simulation. The forcing fields are obtained by linear interpolation to the OGCM time step of monthly-mean CGCM output assigned at half month. To compensate for unrealistic behaviors due to this approximation in long runs, we add a relatively weak (thirty-day) relaxation of surface temperature and salinity to the CGCM climatology. We refer to this sixteen-year OGCM simulation as the CONTROL-CGCM run. On the one hand, our procedure assures consistency between forcing and internal fields in the ocean model. On the other hand, our results will be affected by the "imperfections" in the CGCM simulation. For example, the meridional structure of the simulated ENSO is, in general, "narrower" compared to that in the observation. Next we perform an OGCM experiment by shifting the phase relationship between interannual anomalies and the seasonal cycle of the surface fluxes by half a year, i.e. by applying the anomalous fluxes with a six-month delay. We refer to this run as the SHIFT-CGCM experiment.

The above experiments are repeated using NCEP reanalysis data (corrected by COADS long-term mean) for the period of 1980-1999. The control run in this case is labeled CONTROL-NCEP and the "shifted" run is labeled SHIFT-NCEP.

3. Upper Ocean Response to the "Shift"

Figure 1 shows the monthly-mean temperature anomalies in the upper ocean (0-300 m) along the Equator obtained in CONTROL-CGCM. There are two major ENSO events in this period, of which one is warm (marked as ELN), and one is cold (LAN). The heat content anomalies in the western and eastern parts of the basin during the events appear out-of-phase, typical of observed ENSO events. Figure 2 shows the monthly mean temperature anomalies in the upper ocean at the center of Niño 3 region (Equator, 110^{o} W) in CONTROL-CGCM and SHIFT-CGCM for both ELN and LAN, together with the responses to the "shift". In ELN, the magnitude of the response in heat content anomaly to the "shift" reaches 40% of the maximal anomaly for the event. In LAN, the response of

the heat content anomaly is about half of that in ELN. Responses of this magnitude (20%-40%) can generate coupled atmosphere-ocean interactions that would alter future anomaly evolution if they were allowed by the coupled system.

Before further analysis, we test the persistency of the response we see in the ELN case. We use two methods. In the first one, we make several shorter SHIFT runs (5 years) just for the ELN case but with different "initial conditions". In the ELN case equatorial SST peaks during the second half of Year 4. We restart from spin-up condition at different times in Year 1 and 2 (the 6-month "shift" is always present). In this way the "initial condition" for the warm event would be different due to the varying length of anomalous forcing leading up to the event. As shown in Fig. 3a, this kind of "perturbation" has very little impact on the response to the "shift". In the second test, we simply change the magnitude of the "shift" from 6 months to 3 months and 9 months. The responses to three-month and nine-month "shifts" are just as profound as that to the six-month "shift" (Fig. 3b) even though the details are obviously different.

To produce simple indicators of the basin-wide heat content redistribution in the upper equatorial Pacific during ELN and LAN, we divide the basin into its parts west and east of 150^{o} W. The average and difference temperature anomaly between the two parts define two indices that represent the zonal mean heat content anomaly of the equatorial band and the anomalous zonal tilt of the equatorial thermocline, respectively. Figure 4 shows the time evolution of the two indices in ELN and LAN for both CONTROL-CGCM and SHIFT-CGCM. ELN shows a clear response to the shift in the thermocline tilt index, while LAN shows much smaller response in both indices. The response to the shift, therefore, is very event-dependent on the basin scale. A heat budget analysis for ELN is shown in Fig. 5. It is clear that the change in anomalous zonal advection is almost wholly responsible for the response in eastern basin heat content.

Figure 6 shows the difference between CONTROL-NCEP and SHIFT-NCEP in the same format as Fig. 2. In the panels of Fig. 6 the heat content anomaly is normalized by the maximal values in the closest ENSO events. First, we note that the response to the shift is nonlinear in ENSO amplitude. Second, the response has generally smaller amplitudes

than in the experiments with CGCM surface fluxes. We cannot assess how general this result is due to the short length of available datasets.

4. Detailed Analysis of the ELN Case

In this section we estimate the contribution of "direct or local" and "delayed or remote" effects to the differences between CONTROL-CGCM and SHIFT-CGCM. We focus on October of the fourth year, when the response has the largest magnitude in heat content. First, we perform several October simulations in which the anomalous forcing corresponds to the fourth year of CONTROL-CGCM, but is applied at increasingly earlier times before which the forcings do not have interannual variability. We do this by taking initial conditions from the spin-up run (i.e., obtained without interannual variations in the surface fluxes) corresponding to *n* months before the last October 1 in the spin-up run. These runs are referred to as "CONTROL-*n*" experiments. Next, we repeat the simulations with the seasonal cycle shifted, as we did in the previous section of the paper. This is done by starting the simulations with initial conditions (from the spin-up run) corresponding to *n* months before the last April 1 in the spin-up run, and using exactly the same anomalous surface fluxes. We refer to these runs as "SHIFT-*n*". The larger the "*n*" the more we see the impact of "delayed or remote" effects.

We made 5 pairs of OGCM experiments corresponding to *n*= 1, 3, 6, 9 and 12 (i.e., going back by three months). Figure 7 presents a summary of the results in terms of equatorial anomalous zonal current differences, together with the difference between CONTROL-CGCM and SHIFT-CGCM in October of the fourth year. The panel for *n* = 1 (Fig. 7a) shows that the direct or local response can already explain a part of the difference between CONTROL-CGCM and SHIFT-CGCM in the equatorial mid-basin (Fig. 7f). An inspection of the panel sequence (Figs. 7a to 7e) clearly shows that the difference in the upper 80-100m of the ocean between CONTROL-*n* and SHIFT-*n* increases gradually with *n*. This indicates that the contributions of direct and delayed effects to the difference between CONTROL-CGCM and SHIFT-CGCM are comparable to each other in magnitude.

5. Conclusion

Our study starts with a direct estimation of the impact of upper ocean seasonal variation on an OGCM simulation of ENSO events that were produced by the same model when it was coupled to an AGCM. We examine the impact of shifting by six-month the phase between the seasonally and interannually varying surface fluxes. According to the results, the shift produces differences in eastern basin heat content that can reach 40% of the maximum interannual anomaly in the control run. The response to the shift is also event-dependent. In the major cold event, the same shift has a smaller impact in terms of eastern basin heat content (20%).A heat budget analysis of the warm event shows that the process most affected is anomalous zonal advection in the mid-basin. If the OGCM is forced with surface fluxes corresponding to the NCEP reanalysis for the period 1980-1999, then the response to the shift is still substantial but smaller in magnitude. There are also inter-event variations in the response. Another common feature of the experiments with surface fluxes from the CGCM simulation and NCEP Reanalysis data is that the zonal mean heat content at the Equator is insensitive to the shift (cf. Fig. 4). This indicates that seasonal features such as variation in the advection of heat content anomalies by the WBC into the equatorial band is unimportant or compensated by other processes that counteract such effect because these mechanisms would cause changes in the zonal mean heat content. In view of the short length of available datasets, we cannot assess whether the different responses obtained with CGCM and NCEP surface fluxes is significant. In addition, there are important differences between the mean seasonal cycle simulated by the OGCM with the surface fluxes from the CGCM simulation and NCEP reanalysis.

The ELN case with surface fluxes from the CGCM output is analyzed further to figure out the relative contributions of direct and remote effects to the response. This is done by tracing the impact of anomalous forcing back in time with and without the shift. The results show that the difference between SHIFT-CGCM and CONTROL-CGCM in October of the fourth year increases smoothly as anomalous forcing is applied at increasingly earlier times up to 1 year. This behavior can be interpreted under the "delayed Oscillator" paradigm of ENSO as the following. First we argue that, in this case, both Kelvin waves forced directly in western to central equatorial Pacific, which arrive in

the east 1-2 month later, and Rossby waves reflected at the western boundary and then traveling eastward as Kelvin waves, forced by remote (in time and/or space) anomalous wind forcing, contribute to the response. This then implies that equatorial waves are influenced by the seasonally varying upper ocean mean state in different ways in CONTROL-CGCM and SHIFT-CGCM as they are being forced and propagating in different times of the year. The sum of the differences due to all these contributing wave signals should be what we see in Fig. 2a. There have been many studies (e.g., McPhaden and Ripa, 1990, Giese and Harrison, 1990, Long and Chang, 1992, Zheng et al, 1998) on how features of the equatorial Pacific mean state, can affect equatorially trapped, low-frequency baroclinic Kelvin and Rossby waves. These studies suggest that the SEC/EUC system and its variation can modify vertical structure and phase speed of the waves, and the change in the thermocline slope can also cause changes in the behavior of Kelvin waves.

This further implies that the seasonal variation in the upper ocean can regulate the "delayed oscillator" in the same way as the "coupling instability" (modulated mainly by seasonal variations in the lower atmosphere and oceanic mixed layer mean condition, Tziperman et al, 1998) does. Yang and O'Brien (1993), for example, have shown with an intermediate level coupled model of ENSO that increasing the steepness of the thermocline slope from the central basin to the eastern basin can decrease the interannual variation in their model (and vice versa) due to its impacts on Kelvin wave propagation. In this aspect our results are also consistent with the hypotheses of An and Wang (2001), and Vintzileos et al (1999b).

References

An, S.-I. and B. Wang, 2001: Mechanisms of locking of the El Niño and La Niña mature phases to boreal winter. *J. Climate*, **14**, 2165–2176.

Battisti, D. S., 1988: The dynamics and thermodynamics of a warm event in a coupled atmosphere/ocean model. *J. Atmos. Sci.,* **45**, 2889-2919.

Guilyardi, E., P. Delecluse, S. Gualdi, and A. Navarra, 2003: Mechanisms of ENSO Phase Change in a Coupled GCM. *J. Climate*, **16**, 1141–1158.

Jin, Fei-Fei, 1996: El Niño/Southern Oscillation and the Annual Cycle: Subharmonic Frequency-Locking and Aperiodicity. *Physica D*, **98**, 442-465.

Long, B., and P. Chang, 1990: Propagation of an Equatorial Kelvin wave in a varying Thermocline. *J. Phys. Oceanog.*, **20**, 1826-1841.

McPhaden, M. J., and P. Ripa, 1990: Wave-mean flow interactions in the Equatorial ocean. *Annu. Rev. Fluid Mech.*, **22**, 167-205.

Neelin, J. D., F.-F. Jin, and H.-H. Syu, 2000: Variations in ENSO Phase Locking. *J. Climate*, **13**, 2570-2590.

Tziperman, E., M. Cane, and S. Zebiak, 1998: Locking of El Niño's Peak Time to the End of the Calendar Year in the Delayed Oscillator Picture of ENSO. *J. Climate*, **11**, 2191–2199.

Tziperman, E., S. E. Zebiak, and M. A. Cane, 1997: Mechanisms of Seasonal-ENSO Interaction. *J. Atmos. Sci.,* **54**, 61–71.

Vintzileos, A., P. Delecluse, and R. Sadourny, 1999a: On the mechanisms in a tropical ocean-global atmosphere coupled general circulation model. Part I: mean state and the seasonal cycle. *Climate Dynamics*, **15**, 43–62.

— 1999b: On the mechanisms in a tropical ocean-global atmosphere coupled general circulation model. Part II: interannual variability and its relation to the seasonal cycle. *Climate Dynamics*, **15**, 63–80.

Xie, S.-P., 1995: Interaction between the annual and interannual variations in the Equatorial Pacific. *J. Phys. Oceanog.,* **25**, 1930-1940.

Yang, J., and J. J. O'Brien, 1993: A coupled atmosphere-ocean model in the Tropics with different thermocline profiles. *J. Climate*, **6**, 1027-1040.

Yu, J.-Y., and C. R. Mechoso, 2000: A Coupled Atmosphere-Ocean GCM study of the ENSO Cycle. *J. Climate*, **14**, 2329–2350.

Zheng, Q., R. D. Susanto, X.-H. Yan, W. T. Liu, and C.-R. Ho, 1998: Observation of equatorial Kelvin solitary waves in a slowly varying thermocline. *Nonlinear Processes in Geophysics*, **5**, 153-165.

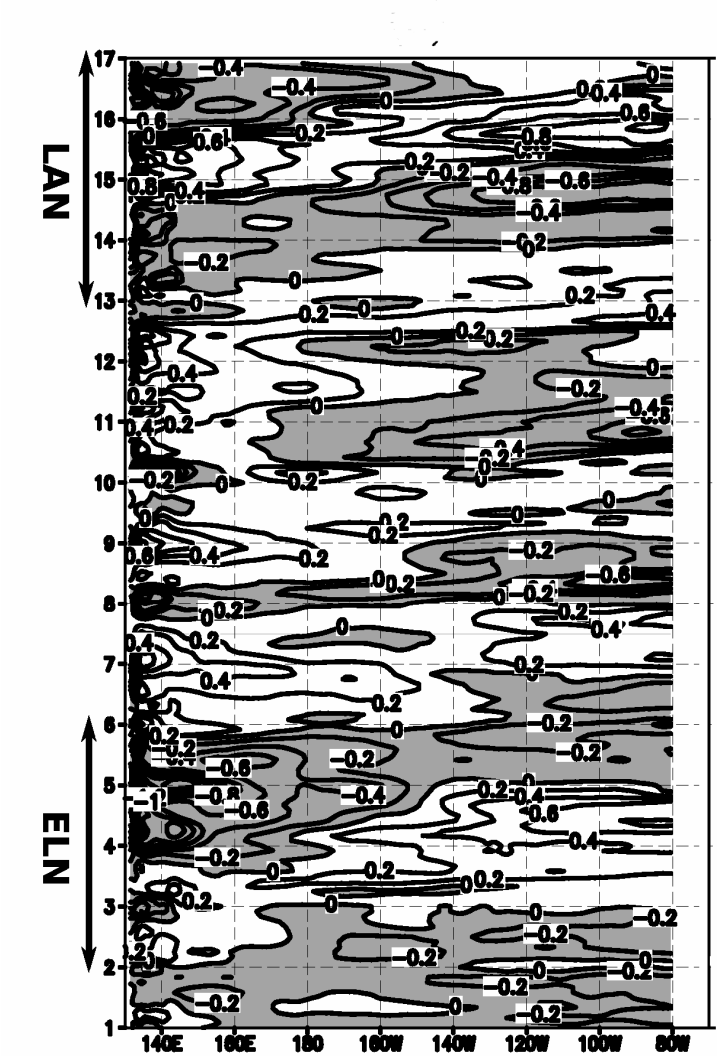

Figure 1: vertical mean temperature anomaly (0~300m) along the Equator (contour interval 0.2^{o}C, negative anomalies shaded). Case ELN and Case LAN are the two major events in this run.

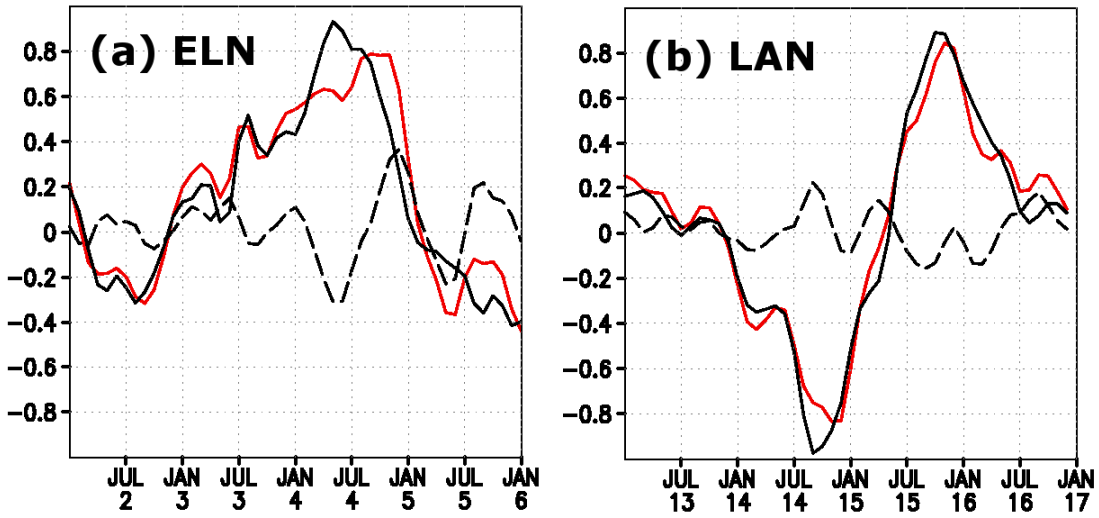

Figure 2: 110°W vertical mean temperature anomaly (0~300m) at the Equator from a) Case ELN, b) Case LAN. The black solid line is for CONTROL-CGCM, the red line for SHIFT-CGCM and the dash line shows the difference between the two. All values are normalized by the maximal monthly anomaly found in the control run.

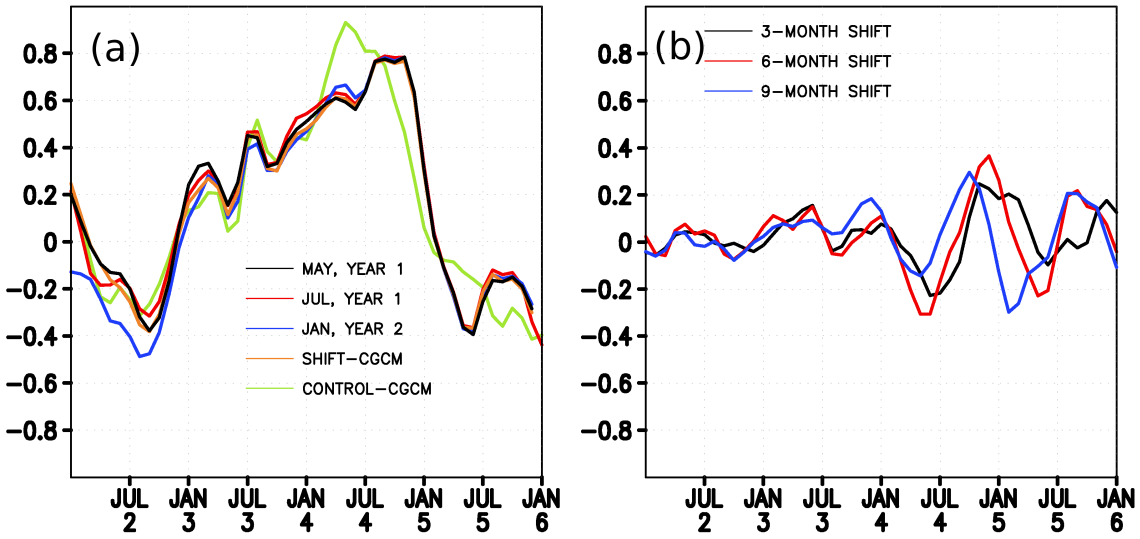

Figure 3: (a) 110°W vertical mean temperature anomaly (0~300m) at the Equator from 5-year runs for case ELN with different restarting point. The same variables from SHIFT-CGCM and CONTROL-CGCM are shown for comparison. (b) responses in the ELN case to "shifts" of 3 months, 6 months and 9 months in terms of 110°W vertical mean temperature anomaly (0~300m) at the Equator.

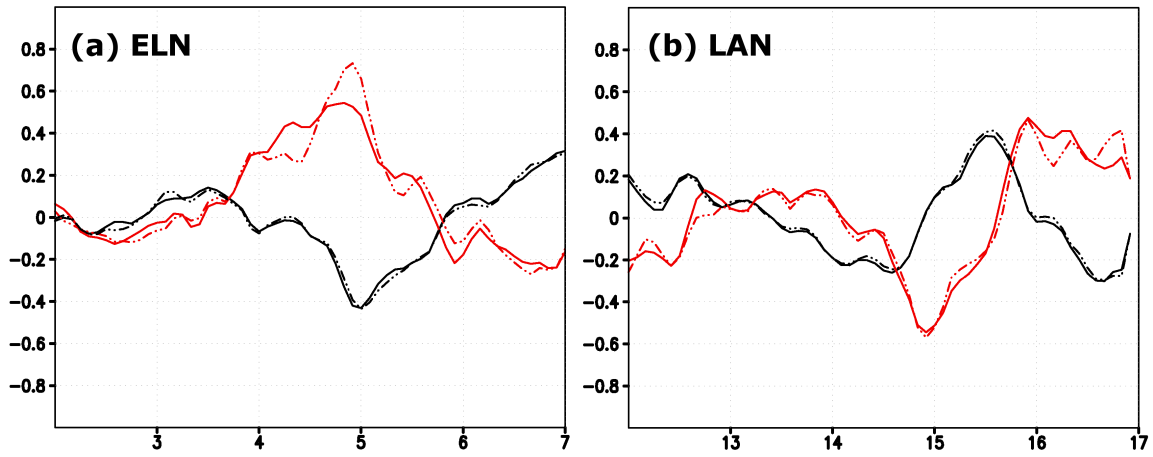

Figure 4: a) The solid and dot-dash lines in red show, the average temperature anomaly (^{o}C) between the eastern and western parts of the equatorial basin (5^{o}S-5^{o}N, 0-300m) for CONTROL-CGCM and SHIFT-CGCM respectively, while the solid and dot-dash lines in black show the difference between the two parts for CONTROL-CGCM and SHIFT-CGCM respectively for case ELN; b) same as a) except for case LAN.

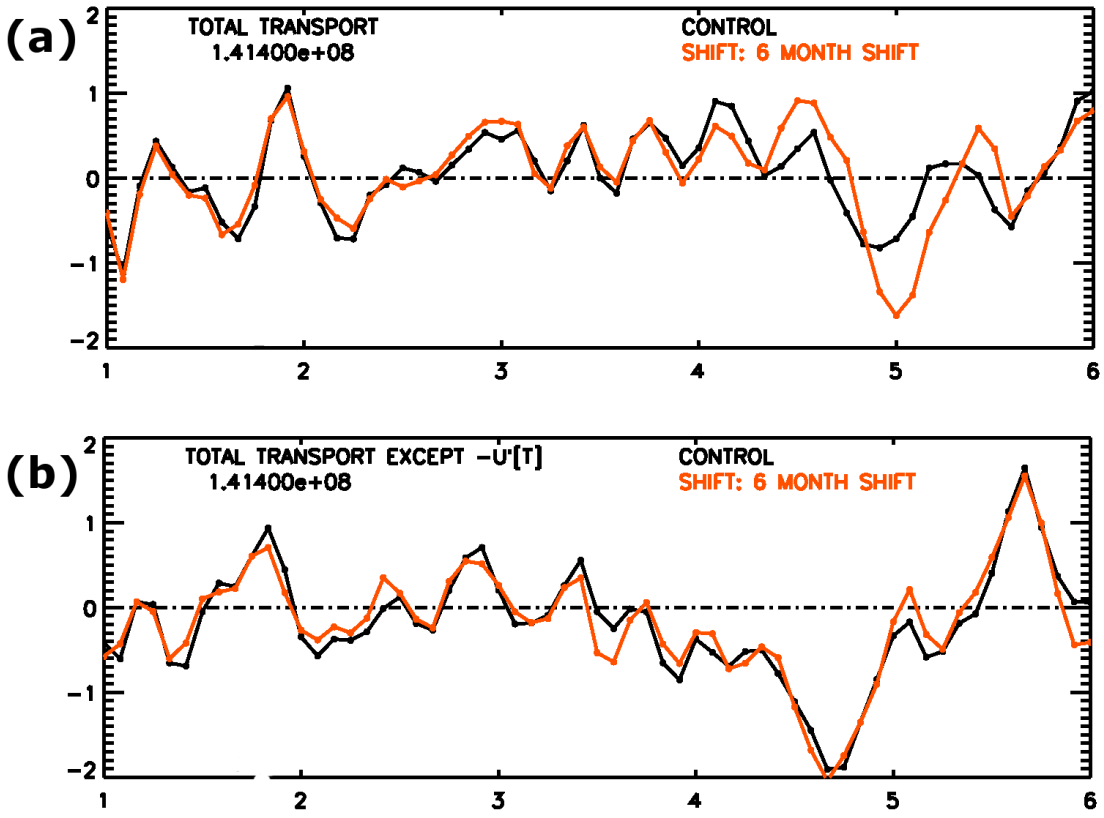

Figure 5: Heat budget analysis for the eastern half of the equatorial band (5°S~5°N, 150°W~70°W, 0~300m) for Case ELN; a) shows the sum of all transport terms in the anomalous heat budget equation (the contribution of surface heat fluxes and heat exchange between the upper ocean and the abyss is omitted) for both CONTROL-CGCM (black) and the SHIFT-CGCM (orange); b) shows in the same format the sum of all transport terms as in a) except for the transport by anomalous zonal advection of mean temperature.

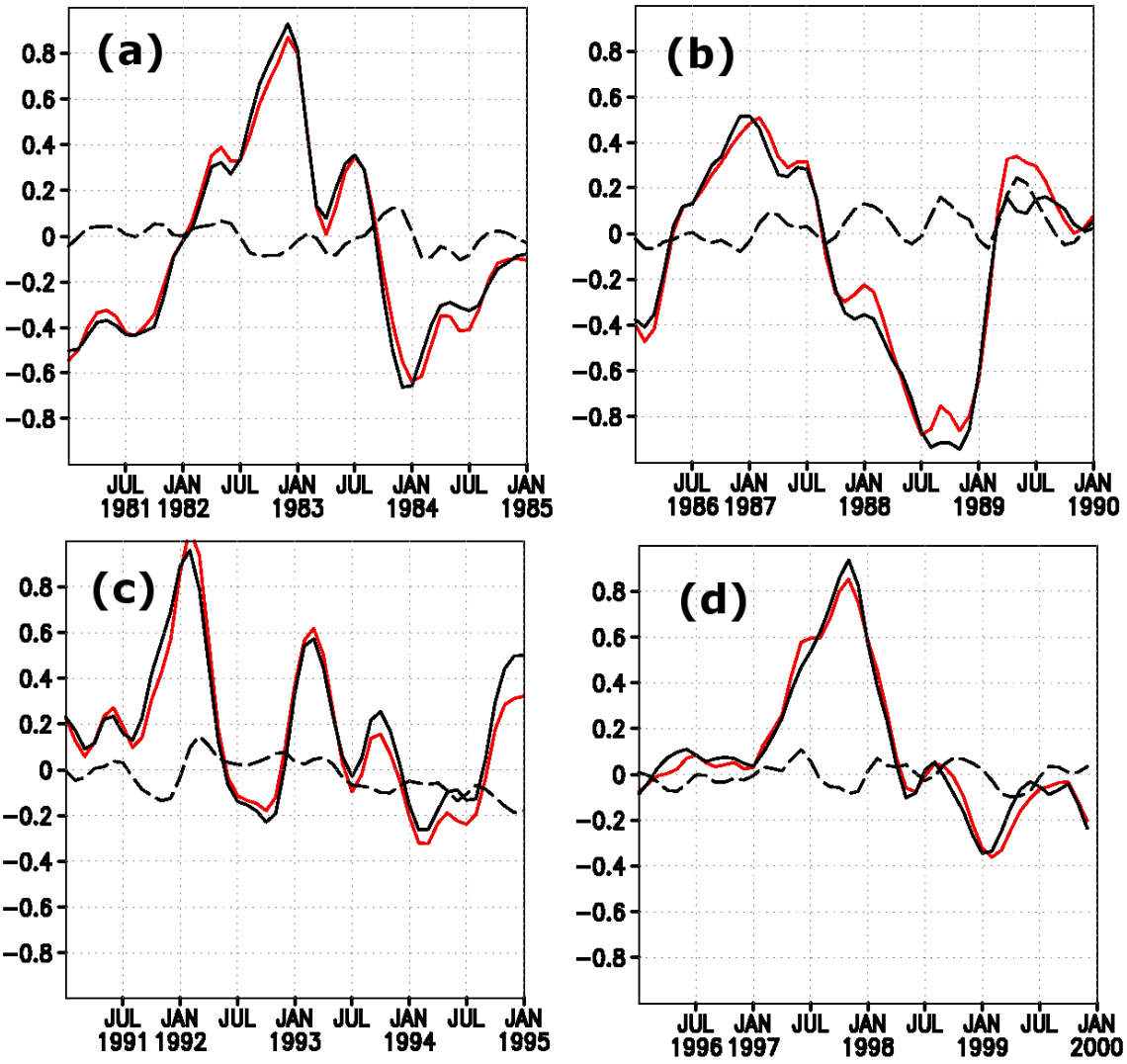

Figure 6: 110°W vertical mean temperature anomaly (0~300m) at the Equator in the same format as Fig. 2 for the period a)1981-1985, b) 1986-1990, c) 1991-1995, d)1996-2000 from CONTROL-NCEP and SHIFT-NCEP. The normalization factor in each panel is the absolute value of the largest anomaly found during the time period.

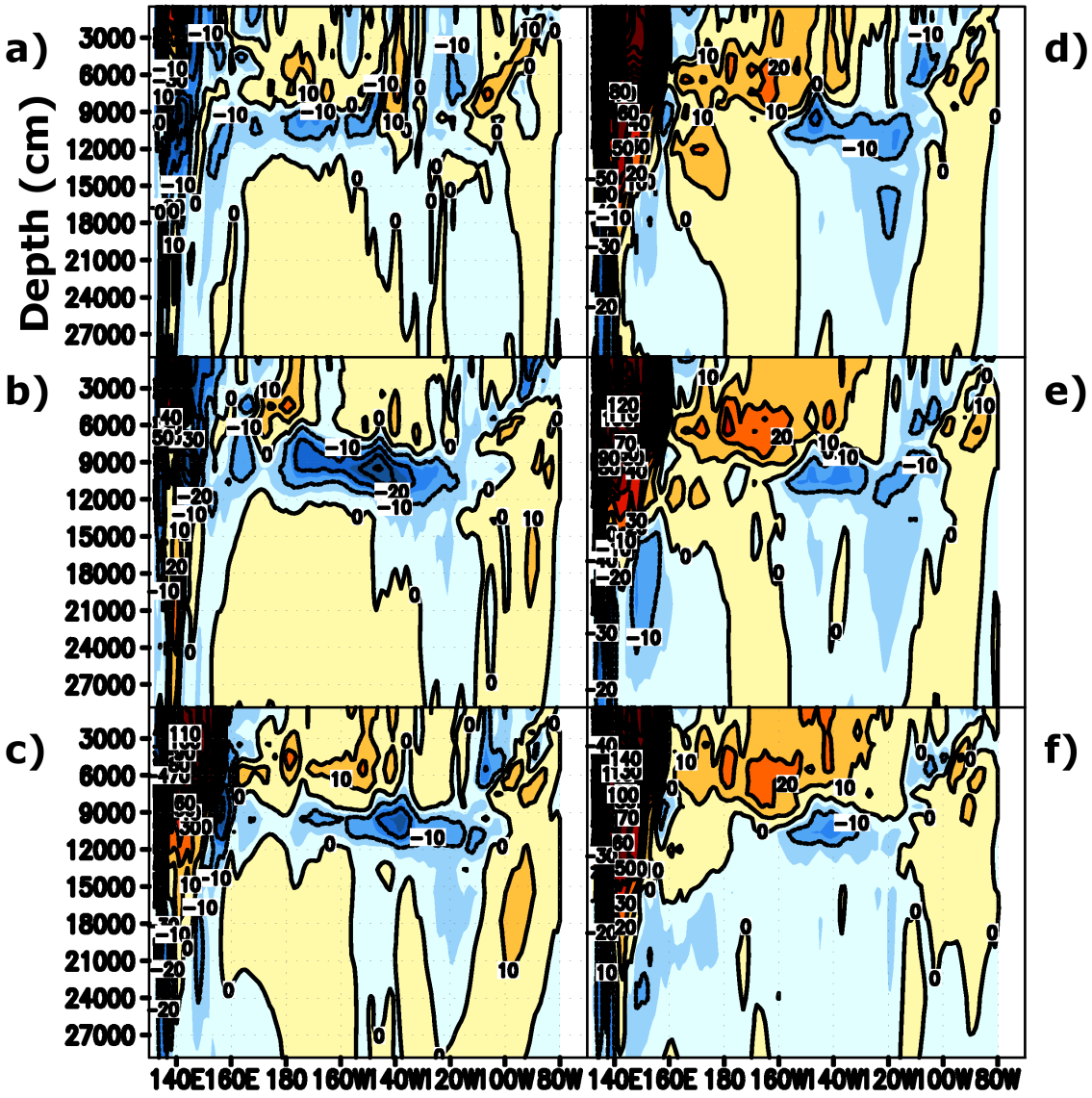

Figure 7: The difference in zonal current anomaly (cm/s, contour interval is 10cm/s) on the Equator for October of the 4th year between a) CONTROL-1 and SHIFT-1, b) CONTROL-3 and SHIFT-3, c) CONTROL-6 and SHIFT-6, d) CONTROL-9 and SHIFT-9, e) CONTROL-12 and SHIFT-12, f) CONTROL-CGCM and SHIFT-CGCM.